

ICNMM2006-96151

MULTI-OBJECTIVE DESIGN OPTIMIZATION OF TOPOLOGY AND PERFORMANCE OF BRANCHING NETWORKS OF COOLING PASSAGES

MAICKEL GONZALEZ¹

Department of Mechanical and Materials Engineering
Multidisciplinary Analysis, Inverse Design, Robust Optimization
and Control (MAIDROC) Lab., EC 3474
Florida International University
10555 West Flagler Street, Miami, FL 33174, U.S.A.
maickel.gonzalez@fiu.edu

RAMON J. MORAL²

Department of Mechanical and Materials Engineering
Multidisciplinary Analysis, Inverse Design, Robust Optimization
and Control (MAIDROC) Lab., EC 3474
Florida International University
10555 West Flagler Street, Miami, FL 33174, U.S.A.
rmora022@fiu.edu

THOMAS J. MARTIN³

Pratt & Whitney Engine Company
Turbine Discipline Engineering & Optimization Group
M/S 169-20
400 Main Street, East Hartford, CT 06108, U.S.A.
thomas.martin@pw.utc.com

DEBASIS SAHOO⁴

Department of Mechanical and Materials Engineering
Multidisciplinary Analysis, Inverse Design, Robust Optimization
and Control (MAIDROC) Lab., EC 3474
Florida International University
10555 West Flagler Street, Miami, FL 33174, U.S.A.
debasis.sahoo@fiu.edu

GEORGE S. DULIKRAVICH⁵

Department of Mechanical and Materials Engineering
Multidisciplinary Analysis, Inverse Design, Robust Optimization
and Control (MAIDROC) Lab., EC 3474
Florida International University
10555 West Flagler Street, Miami, FL 33174, U.S.A.
dulikrav@fiu.edu Web page: <http://maidroc.fiu.edu>

NENAD JELISAVCIC⁶

Department of Mechanical and Materials Engineering
Multidisciplinary Analysis, Inverse Design, Robust Optimization
and Control (MAIDROC) Lab., EC 3474
Florida International University
10555 West Flagler Street, Miami, FL 33174, U.S.A.
njeli001@fiu.edu

ABSTRACT

The objective of this study was to develop an automatic, self-sufficient, preliminary design algorithm for optimization of topologies of branching networks of internal cooling passages. The software package includes a random branches generator, a quasi 1-D thermo-fluid analysis code COOLNET, and a multi-objective hybrid optimizer. COOLNET analysis software has the same trends as shown in an earlier publication depicting the results of a similar analysis code used by Pratt & Whitney. The hybrid multi-objective optimization code was verified against classical test cases involving multiple objectives. The number of branches per level was optimized in order to minimize

coolant mass flow rate, total pressure drop, and maximize total heat removed.

Optimization with four levels of fractal branching channel networks was tested. This optimization varied the number of branching channels extending from each single channel. COOLNET needed approximately forty iterations on average to analyze each configuration. The number of iterations necessary for each geometry depended on the number of branches per configuration. The hybrid multi-objective optimizer needed 500 iterations to create a converged Pareto front of optimized branching network configurations for the case of four branching levels. A population of 60 designs was used. The total number of function evaluations analyzed was 30,000. The entire design optimization process takes approximately 3 hours on a single 3.0 GHz Pentium IV processor.

In this work the total number of Pareto-optimal designs was 100. After finding the Pareto front points, the user has to decide which optimized cooling network configuration is the best for the desired application. It was demonstrated that this can be accomplished by utilizing Pareto-optimal solutions to

¹Graduate student. Currently with Cessna Aircraft.

²Graduate student.

³Senior systems design engineer. Member ASME.

⁴Graduate student.

⁵Professor and Chairman, MME Department.

Director of MAIDROC. Fellow ASME.

⁶Graduate student. Student member ASME.

create a curve representing pumping power vs. total heat removed and by observing which designs provide favorable break-even energy transfer. The magnitude of the ratio of heat transferred to total pressure drop and ratio of heat transfer to pumping power could be further increased by incorporating the channels' hydraulic diameter, cross sectional area, lengths, and wall roughness as optimization variables.

INTRODUCTION

A fractal branches generator program was created to obtain a network of fractal branching channels in a random fashion. This program was written in the Fortran programming language and it allows having a different fractal branching geometry every time the program runs. The network consists of two possible scenarios. One is a diverging branching network, similar to the roots in a tree, and the other is a diverging-converging branching network, similar to the veins and arteries in the human body. In this work only the diverging fractal branching network was used. Each configuration was allowed to randomly contain multiple exits and one inlet. The internal fluid flow properties through the branching geometry were solved with a quasi one-dimensional, finite element, thermo-fluid flow network analysis program and the whole geometry of the system was optimized.

In the quasi one-dimensional, finite element, thermo-fluid flow network analysis program COOLNET [1-3], written in the Fortran programming language, semi-empirical correlations were used to determine the coolant heat transfer coefficients, h_c , while the quasi one-dimensional momentum and enthalpy equations were solved for the total pressure losses and bulk coolant temperatures, $T_{t,c}$, of the coolant fluid. The heat transfer coefficients and bulk coolant temperatures were assumed to vary in the coolant flow direction.

Each fluid element had two nodal endpoints. Each internal node needed to have at least one path entering it (source) and one or more paths leaving (sink). Those nodes that had no sources but had one or more sink paths indicated a supply path. Those nodes connected to one or more sources, but having no sink paths were called a dump path (exit).

COOLNET [1-3] predicted coolant flow rate, \dot{m} , total coolant pressures, P_t , bulk coolant total temperatures, $T_{t,c}$, and internal heat transfer coefficient distributions, h_c , inside internally cooled objects. The program was written as a generalized finite element program [4-6] for thermo-fluid elements. The properties of connecting elements like the cross-section areas, hydraulic diameters, and element lengths were calculated based on suggestions made by West et al [15] for two dimensional flow networks. Then, network connections were optimized by allowing the number of branching elements per node to vary from one to five in order to maximize the total amount of heat removed by the coolant fluid, minimize the coolant mass flow rate, and minimize the total pressure drop of the coolant. This amounted to a total of 31 design variables with three design objectives for the case of 4 branching levels.

A hybrid multi-objective optimization algorithm, [7], capable of dealing with several objective functions simultaneously in a Pareto front optimal sense, was used to perform the optimization process. The hybrid optimization algorithm includes multi-objective versions of three evolutionary optimization algorithms, these are: non-dominated sorting differential evolution (NSDE), [8], strength Pareto

evolutionary algorithm (SPEA), [9], and a multi-objective particle swarm (MOPSO) algorithm based on particle swarm, [10]. An automatic switching algorithm was created [7] to switch among the three multi-objective algorithms [11] during the optimization in order to avoid any stalling or meandering of successive Pareto front approximations. All the calculations were performed in the MAIDROC laboratory cluster [12].

A multi-objective optimizer allows for more design variables and objectives to be specified for the optimization. The optimized design variables, together with a new fractal branching geometry, are used as new input for COOLNET to obtain the best total heat removed, pressure drop, and coolant flow rate. As the result of the optimization, Pareto front points are obtained.

NOMENCLATURE

C_p	Specific heat of coolant
d_k	Hydraulic diameter of a channel in segment k
D	Euclidean dimension
h_c	Heat transfer coefficient on internal surfaces
L_k	Length of a channel in segment k
L_m	Terminal channel length
L_{tot}	Total channel length
\dot{m}	Mass flow rate in a coolant passage
m	Total number of branching levels exclusive of 0 th level
n	Number of branches into which a single channel splits
P_t	Total pressure in coolant fluid system
ΔP_t	Total pressure drop
\dot{Q}	Total heat removed
$T_{t,c}$	Bulk total temperature of coolant
Greek letters	
β	Branching diameter ratio
γ	Branching length ratio
ρ	Density of coolant

PHYSICAL AND MATHEMATICAL MODEL

The shape of the initial cooling passages is an internal network of fractal branching channels and it is presented in Figure 1.

This initial configuration has 1 inlet and 125 exits, and the main flow path splits at each intersection. All nodes are evenly spaced across a maximum width of 0.03 m. In Figure 1 the flow direction is shown to represent how the coolant fluid moves through the fractal branching network. Element properties like cross sectional areas, hydraulic diameters, and lengths are calculated using the scaling laws of West *et al.* [15].

The computer program used to analyze the cooling properties of the initial configurations shown in Figure 1 also can account for micro ribs, staggered and inline rows of pin fins and impingement holes, but these features were not used in this work.

The internally cooled object involves a network with many branches and various types of connections that could be easily developed by using the branches generator with variable number of connections between the nodes.

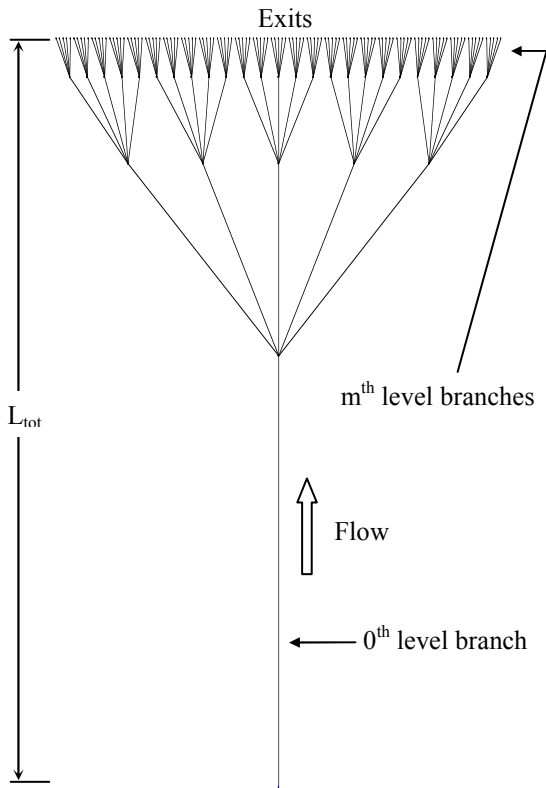


Fig. 1: Geometry of initial cooling configuration with 4 branching levels depicting direction of coolant flow, inlet and exits.

Each fluid element (a member of the cooling network which connects two nodes) can have different wall roughness, angle, length, cross sectional area and geometry. Local hydrodynamic losses were computed in each fluid element based on the local value of the Reynolds number.

The scheme of Figure 1 is used for calculation in this work and it is optimized to give the best cooling performance by allowing the number of branches developing from a single channel to vary from 1 to 5 while keeping all other element properties such as; channel lengths, cross-sectional areas, hydraulic diameter, and wall roughness fixed. For more general calculations this network can be developed with other geometries, with different arrangement of connections between the nodes, different number of nodes, different number of elements, etc.

In Figure 1 each node is represented by the intersection where one or more lines join and each element is a line connecting two nodes. The coolant flow enters through the inlet and exits through all the exits. The internal coolant network was sub-divided into kk elements (fluid paths). Fluid elements were connected, as presented in Figure 1, between nn nodes. The number of inlet and exit nodes, mm , was included in the total number of nodes, nn .

Each fluid element has two nodal endpoints (inlet and exit). Internal nodes have at least one path entering it (source) and one or more paths leaving (sink). Nodes that have no sources, having one or more sink paths indicate a supply (inlet) path. Similarly, nodes connected to one or more sources, having no sink paths are called a dump (exit) path.

CREATING THE NETWORK GEOMETRY

Geometric information of the internal coolant passages was accomplished by using the scaling laws found in the work of West *et al.* [15] for two dimensional branching channel networks. These scaling laws give the branching diameter and lengths ratios.

$$\beta = \frac{d_{k+1}}{d_k} = n^{-\frac{1}{D+1}} \quad (1)$$

$$\gamma = \frac{L_{k+1}}{L_k} = n^{-\frac{1}{D}} \quad (2)$$

The symbol γ represents the branching length ratio, β represents the branching diameter ratio, m indicates the total number of branching levels exclusive of 0^{th} level which is the inlet of the branches, n represents the number of branches into which a single channel branches, D is the Euclidean dimension, d_k represents the hydraulic diameter of a channel in segment k , and L_k represents the length of a channel in segment k , where k is indexed from *zero* to m .

Specifying a total channel length L_{tot} and using the relation

$$L_m = \frac{L_{tot}}{\sum_{i=0}^m \frac{1}{\gamma^i}} \quad (3)$$

to find the terminal channel length L_m , allows to calculate the length of all the branching levels by using equation (2). In a similar fashion all the hydraulic diameters are calculated using equation (1) given the hydraulic diameter of any branching level.

The random braches generator was initialized as shown in Figure 1, to five branching channels extending from each channel, $n = 5$, four branching levels, $m = 3$ (excluding the 0^{th} level), for a two dimensional object, $D = 2$, the total channel length $L_{tot} = 0.06$ meters, and an inlet hydraulic diameter of $d_{k=0} = 2.006 \times 10^{-3}$ meters.

Table 1 below illustrates the values to which channels in each level were initialized using the diameter and length ratios calculated before. Other initialization parameters were the interior wall roughness and the wall surface temperature for each channel; these initial values are 0.3175×10^{-3} m and 1025 K, respectively. The interior wall roughness was kept constant for all the elements in the fractal branching network. The boundary conditions at the inlet were a total pressure of 1.7066×10^6 Pa and a total temperature of 893.37 K. The boundary conditions at the exits were a static ambient pressure of 7.5289×10^5 Pa and a static temperature of 1366.4 K.

k	A_k (m)	$d_{H,k}$ (m)	L_k (m)
0	1.504×10^{-4}	2.006×10^{-3}	3.455×10^{-2}
1	8.795×10^{-6}	1.173×10^{-3}	1.545×10^{-2}
2	5.144×10^{-6}	6.860×10^{-4}	6.910×10^{-3}
3	3.008×10^{-6}	4.012×10^{-4}	3.090×10^{-3}
		Total	6.000×10^{-2}

Tab. 1: Geometry dimensions for channels of Figure 1.

OPTIMIZATION WITH COOLNET

The hybrid-multi-objective optimizer combined with the fractal branches generator and COOLNET is used to optimize the internal passage geometry for optimum flow properties and geometry. Program OBJ is written as the connection between the branches generator, COOLNET and the hybrid multi-objective optimizer. Program OBJ, which is called by the optimization algorithm performs the following tasks:

- Reads branching generator's initial input file.
- Reads optimizer's output file.
- Writes new branches generator's input file based on optimizer's output file.
- Runs the branches generator program.
- Branches generator writes COOLNET's input file.
- Runs COOLNET using input given by branches generator.
- Reads total number of elements from COOLNET's input file.
- Reads COOLNET's output file.
- Calculates objectives.
- Writes input file for optimizer.

With the last step, the optimizer makes decisions and the process repeats in a loop until the desired number of function evaluations is reached.

The design variables in this research are the number of branching channels allowed to propagate from a single channel. For all the channels the number of developing branching channels was allowed to vary from 1 to 5. Table 2 summarizes the number of design variables and the range these variables are allowed to change for a network with 4 branching levels. The column labeled Number refers to the total number of design variables being optimized. The columns labeled Min and Max refer to the minimum and maximum number these variables can adopt while in the optimization process. For the four branching levels configuration the values in Table 1 were kept constant.

Configuration	Number	Min	Max
Four Branching Levels	31	1	5

Tab. 2: Design variables.

Table 3 lists the optimization objectives in this research. These objectives were maximized or minimized accordingly as to obtain the best branching geometry. The column labeled Objective Name refers to the desired objective, and Minimized or Maximized refers to how the objective is optimized, either by minimizing or maximizing it.

Objectives are as follow:

- Total heat removed – is the heat, which the coolant absorbs from the walls per unit time.
- Total pressure drop – is the total pressure difference between inlet and the exits.
- Mass flow rate – is the total mass flow of the coolant per unit time.

Objective Name	Minimized	Maximized
Total heat removed		x
Total pressure drop	x	
Mass flow rate	x	

Tab. 3: Optimization objective.

RESULTS

During the optimization process different configurations are developed and tested by the optimization program. Those that produce satisfactory results in terms of the three objectives are used to predict a better configuration in the next function evaluation. After each function evaluation, the Pareto front, which is a three dimensional graph of values of the three objectives as configurations change, moves until the solution reaches a steady state where no other better solution is feasible, and at this instance optimized points remain in the same configuration without changing. This means that the final shape of the Pareto front is reached and that the optimization process is finished. When the final shape of the Pareto front is reached, then the designer can decide and analyze which point is the best for the desired needs. In this work choosing the configuration that requires the least amount of pumping power is of great importance.

For this particular optimization process there were three objectives, this is the reason why the Pareto front graph is three dimensional, each axis on the graphs presented in the following figures represents one objective. Each optimal point in the figures that follow has three coordinates. These coordinates are:

- Total heat removed with units of Watts, plotted in the x-axis.
- Total pressure drop of the coolant with units of bars, plotted in the y-axis.
- Mass flow rate of the coolant with units of kilograms per second, plotted in the z-axis.

In the following figures a two dimensional view of the Pareto front is presented in order to observe the changes of the three objectives with respect to each other as the optimization process progresses from start to end. These views of the Pareto front show all the optimized points from the particular viewing axis. The diamond shown in all the figures of the Pareto front corresponds to the value of the three objectives for the initial configuration of Figure 1. The objective values for the initial configuration are shown for comparison purposes. The optimization process requires approximately 3 hours on a 3.0 GHz Pentium IV processor.

The following results show a sequence of optimized points at various stages in the optimization process. These results are related to the initial configuration shown in Figure 1 for 4 branching levels. Figures 2 through 4 represent optimal designs after the first iteration. Figure 2 shows the relation between total heat removed and mass flow rate. Total heat removed and mass flow rate are linearly related by the formula

$$\dot{Q} = \dot{m} c_p \Delta T \quad (4)$$

and this linear relation is observed in Figure 2. During the first function evaluation the optimizer found 28 possible configurations out of 100, which is the pre-specified number of Pareto points for this optimization.

Figure 3 shows the relation between total heat removed and pressure drop. Figure 4 shows the relation between pressure drop and mass flow rate. Figure 5 shows one of the possible geometric configurations based on a point on the Pareto front where the heat removed is 548.54 W, the pressure drop is 2.0031 bars, and the mass flow rate is 0.0097044 kg/s.

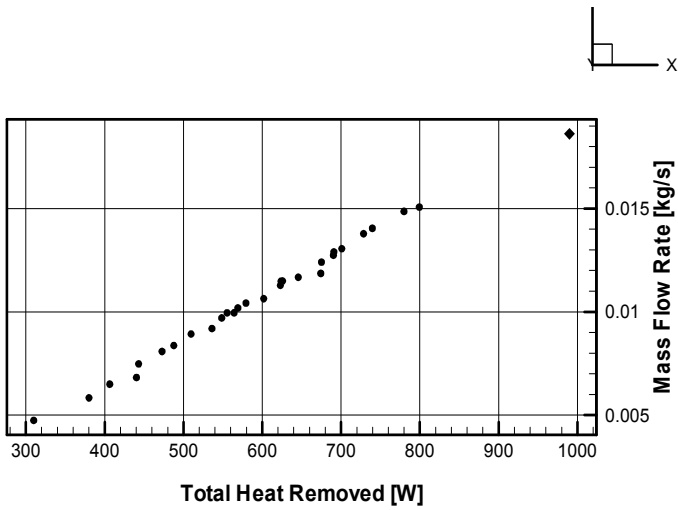


Fig. 2: Optimal points after 1st iteration, $\dot{Q} - \dot{m}$ view.

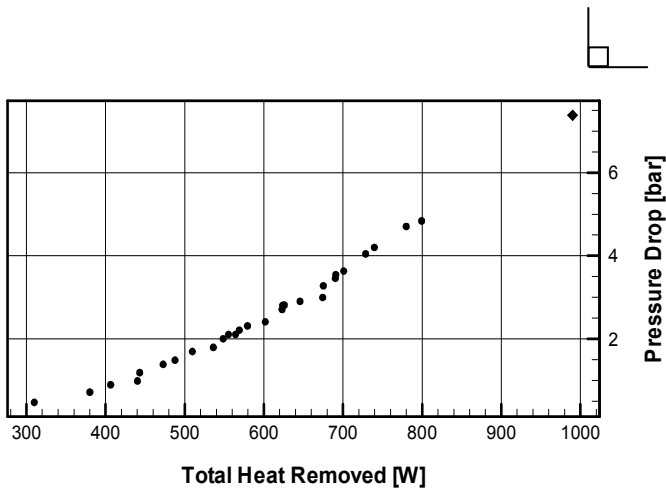


Fig. 3: Optimal points after 1st iteration, $\dot{Q} - \Delta P_t$ view.

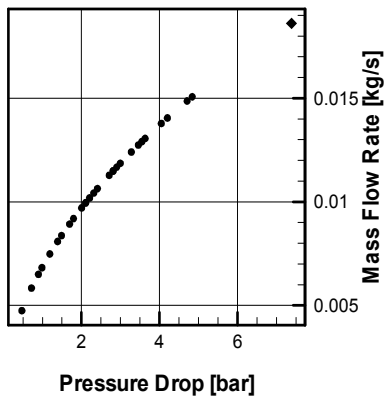


Fig. 4: Optimal points after 1st iteration, $\Delta P_t - \dot{m}$ view.

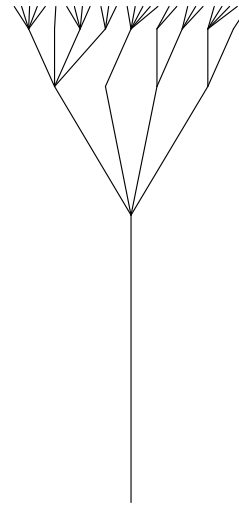


Fig. 5: View of one possible configuration after 1st iteration.

Figures 6 through 8 represent the two-dimensional views of optimal designs after 167 iterations. Figure 6 shows the relationship between total heat removed and mass flow rate. Here too, the linear relationship between total heat removed and mass flow rate is observed. Figure 7 shows the relationship between total heat removed and pressure drop.

Figure 8 shows the relationship between pressure drop and mass flow rate. The number of Pareto points is 100 and this number is specified in the input file for the optimizer, this means that the optimizer can find 100 optimal configurations based on the desired objectives. Figure 9 shows one of the possible geometric configurations based on a point on the Pareto front where the heat removed is 536.12 W, the pressure drop is 1.4786 bars, and the mass flow rate is 0.0083426 kg/s.

Figures 10 through 12 represent optimal designs after 334 iterations. Figure 10 shows the relationship between total heat removed and mass flow rate. The linear relationship between total heat removed and mass flow rate is also observed.

Figure 11 shows the relationship between total heat removed and pressure drop. Figure 12 shows the relationship between pressure drop and mass flow rate.

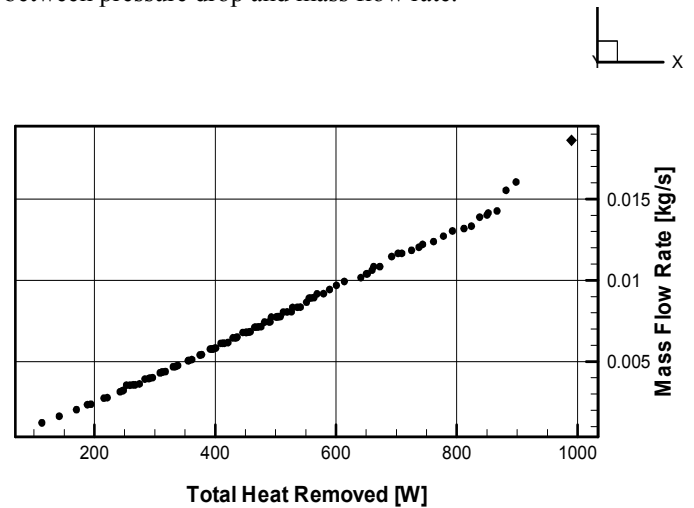


Fig. 6: Optimal points after 167 iterations, $\dot{Q} - \dot{m}$ view.

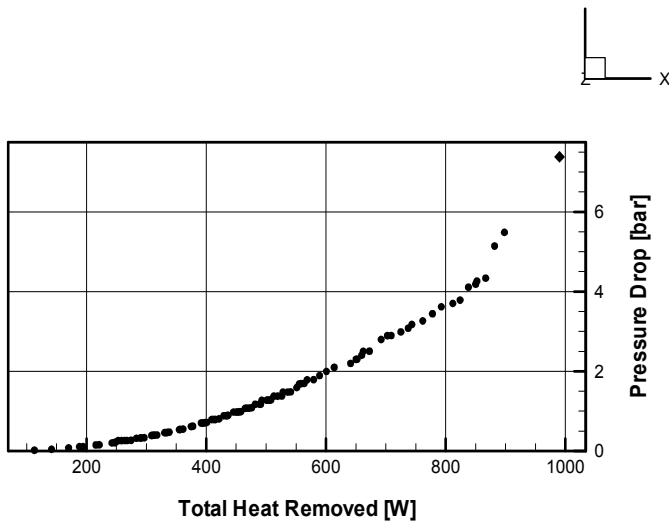


Fig. 7: Optimal points after 167 iterations, $\dot{Q} - \Delta P_t$ view.

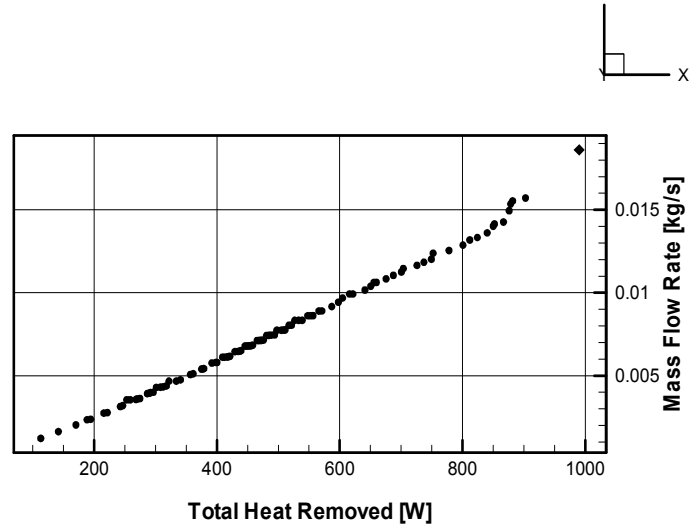


Fig. 10: Optimal points after 334 iterations, $\dot{Q} - \dot{m}$ view.

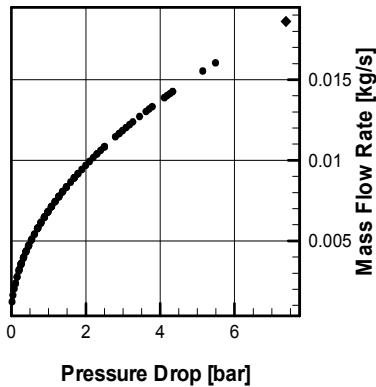


Fig. 8: Optimal points after 167 iterations, $\Delta P_t - \dot{m}$ view.

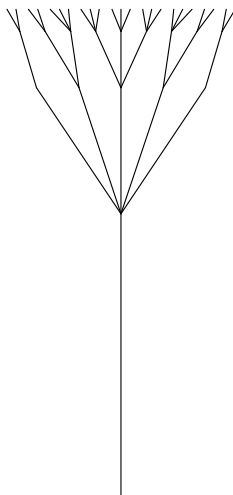


Fig. 9: View of one possible configuration after 167 iterations.

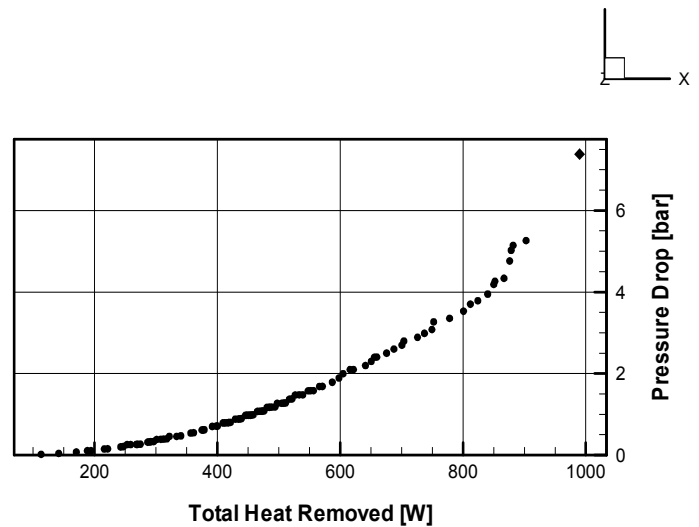


Fig. 11: Optimal points after 334 iterations, $\dot{Q} - \Delta P_t$ view.

The number of Pareto points is 100; therefore, there are 100 possible designs which is the result of a truly multi-objective optimization. If a linear combination of the single objectives was optimized, it would involve user-specified weighting factors thus creating only a single point on the Pareto surface where this point would depend on the chosen weights.

The diamond symbol represents the objective values for the initial configuration, which is the highest achievable for this case. Figure 13 shows one of the possible flow geometries based on a point on the Pareto front where the heat removed is 615.9 W, the pressure drop is 2.0976 bars, and the mass flow rate is 0.0099301 kg/s.

Figures 14 through 16 represent optimal designs after 500 iterations. The optimization was stopped at this stage because there was little change in the shape of the Pareto front as can be observed by comparing Figures 10 through 12 and 14 through 16. Figure 14 shows the relationship between heat transfer and mass flow rate.

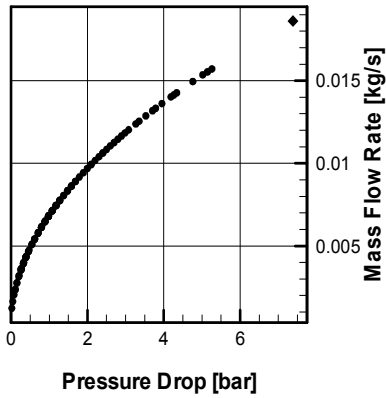


Fig. 12: Optimal points after 334 iterations, $\Delta P_t - \dot{m}$ view.

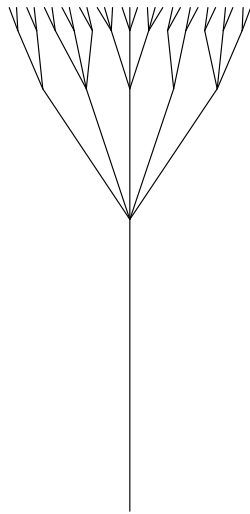


Fig. 13: View of one possible configuration after 334 iterations.

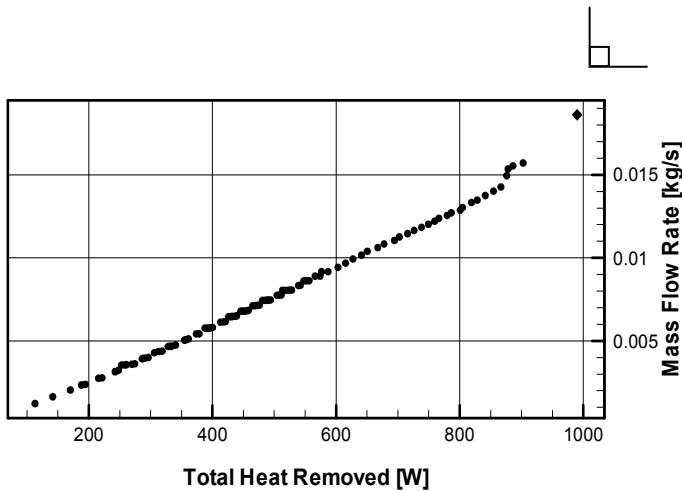


Fig. 14: Optimal points after 500 iterations, $\dot{Q} - \dot{m}$ view.

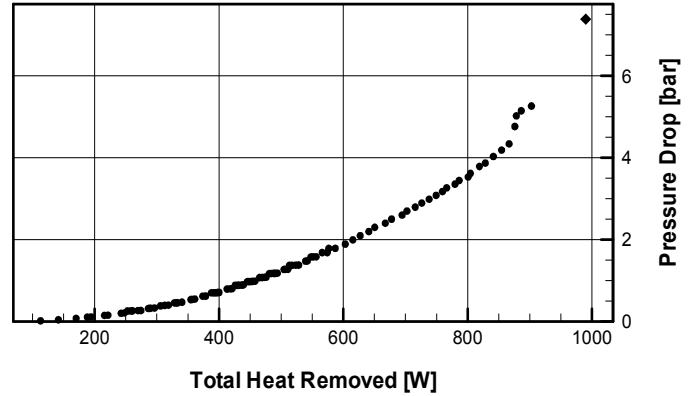


Fig. 15: Optimal points after 500 iterations, $\dot{Q} - \Delta P_t$ view.

Figure 15 shows the relationship between heat transfer and pressure drop.

Figure 16 shows the relationship between pressure drop and mass flow rate. Figure 17 shows one of the possible geometric configurations based on a point on the Pareto front where the heat removed is 523.56 W, the pressure drop is 1.3765 bars, and the mass flow rate is 0.0080506 kg/s. These are now the final optimized values of the three objectives and are ready for analysis. Here there are 100 different configurations to choose from. The analysis is performed in the next section.

For comparison purposes the number of optimization iterations was increased to 1000 to confirm that the Pareto front was at its most optimized shape. It was noted that very minor changes occurred near the upper-right-hand corners of Figures 14 through 16. Since the changes in the Pareto front were very concentrated and only in one far extreme it was determined that 500 iterations are a good point to stop the optimization process.

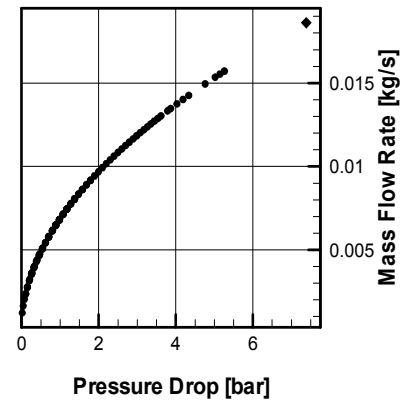


Fig. 16: Optimal points after 500 iterations, $\Delta P_t - \dot{m}$ view.

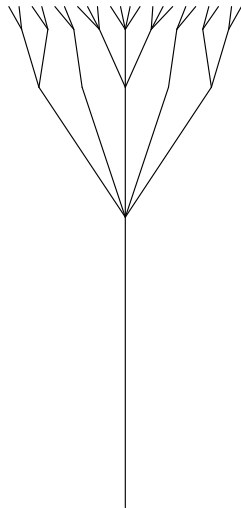


Fig. 17: View of one possible configuration after 500 iterations.

ANALYSIS OF RESULTS

The final results are going to be analyzed here in order to get the best design using 4 branching levels. Only those optimum points obtained after 500 iterations are considered. The population was 60, thus the total number of function evaluations was 30000. The number of Pareto points was 100, thus the number of optimal designs obtained from the optimization is 100.

For the analysis, the optimized objectives were compared to the calculated values of total heat removed, total pressure drop, and mass flow rate of the initial configuration shown in Figure 1. These values were taken as reference and are shown in Table 4.

\dot{Q}_{ref} [W]	ΔP_{tref} [bar]	\dot{m}_{ref} [kg/s]
990.02	7.3820	0.018614

Tab. 4: Reference objective values for the case of 4 branching levels.

To determine the best design from the data presented in Figures 14 through 16 it is necessary to plot the ratio of total heat removed to pumping power, $\frac{\dot{Q}_{avg}}{\Delta P_t \dot{m}}$, as a function of total

heat removed, \dot{Q} . To obtain this ratio it is necessary to convert the units of total pressure drop from bars to Pascals. The units of total heat removed remain in Watts and the units of mass flow rate remain in kilograms per second. The best design is the one where the total heat removed to pumping power ratio is the highest among the other designs. This ratio must be the highest because the objective is to remove as much heat as possible with the least amount of pumping power.

In Figure 18 the single diamond symbol represents the total heat removed to pumping power ratio of the initial configuration and the circles represent the same ratios for all the Pareto points in Figures 14 through 16.

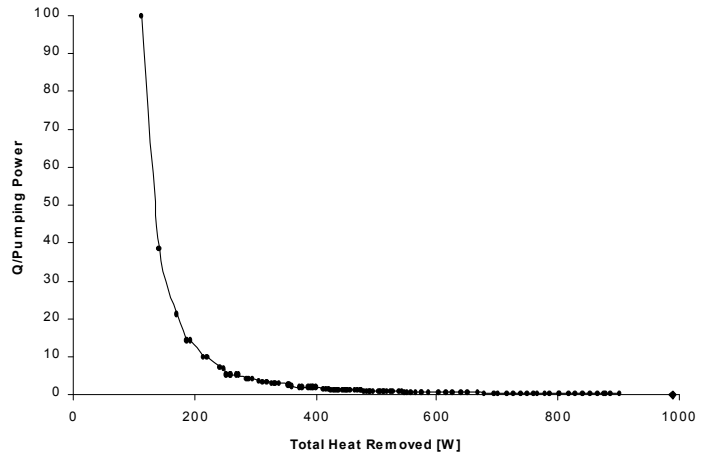


Fig. 18: Ratio of total heat transfer vs pumping power as a function of total heat removed.

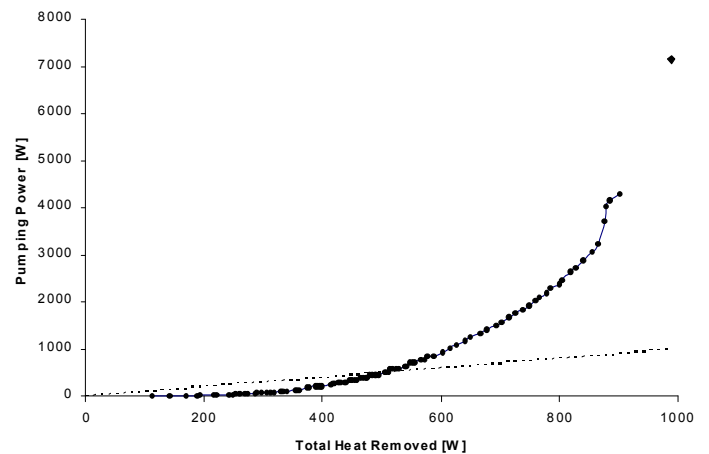


Fig. 19: Pumping power vs. total heat removed.

Figure 19 shows the pumping power necessary to drive the cooling fluid through the network plotted as a function of total heat removed. The dotted line in Figure 19 represents the values that would exist if the pumping power would be equal to the total heat removed, meaning that for one Watt of power needed to drive the flow, one Watt of heat is removed by the coolant. All the points below the dotted line are good solutions, because the power needed to pump the coolant is less than the amount of total heat removed. All the points above the dotted line are the unfavorable solutions, because more power is needed for pumping than the amount of heat removed.

Note that the initial configuration, which is represented by the diamond, falls in the unfavorable region. All the points plotted in Figure 19 are arranged from left to right in the same ascending order of Pareto points in Figures 14 through 16. Therefore, the left most point corresponds to Pareto point 1 and the right most point corresponds to Pareto point 100. The diamond corresponds to the initial configuration.

Figure 20 below is a magnification of the favorable region of Figure 19, which consists of all the values of pumping power vs. total heat removed under the dashed line. In Figure 20 all

the Pareto points from 1 through 56 are represented starting with the value of pumping power vs. total heat removed of Pareto point 1 in the left most point and concluding with the value of pumping power vs. total heat removed of Pareto point 56 in the right most point.

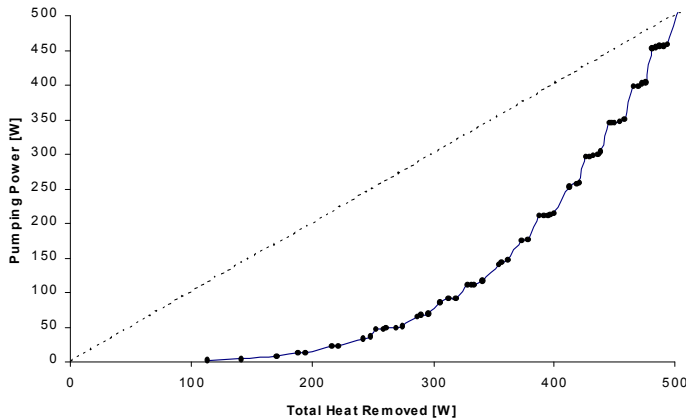


Fig. 20: Magnification of a section of Figure 19.

The optimization objectives were to simultaneously maximize the total heat removed, minimize the total pressure drop, and minimize the mass flow rate.

Now, the focus is to select from Figure 18 the point with maximum ratio of the total heat removed to pumping power. The point with the highest ratio is beneficial because it is desired to remove the maximum amount of heat while minimizing the total pressure drop; also it is desired to remove the maximum amount of heat while minimizing the pumping power required to circulate the coolant fluid. From Figure 18 the point with the highest total heat removed to pumping power ratio corresponds to Pareto point 1. However, Pareto point 1 provides the smallest total heat removed, smallest total pressure drop, and smallest mass flow rate. Consequently, this point also has the best total heat removed to pressure drop ratio and the best total heat removed to pumping power ratio. Greater detail of the amount of pumping power necessary to move the coolant flow and the amount of total heat removed for the configuration of Pareto point 1 is observed in Figure 20

The values of total heat removed, \dot{Q} , coolant total pressure drop, ΔP_t , and coolant mass flow rate, \dot{m} , at Pareto point 1 are 112.94 W, 0.0177 bars, and 0.0012265 kg/s, respectively. Figure 21 below is the geometric configuration of the fractal branching channel associated with Pareto point 1. This figure shows the branches orientation only, parameters like the cross-sectional area, hydraulic diameter, and branching level lengths remained fixed for each branching level as described in Table 1. In Figure 21, the first branching level which is the inlet, has one channel, while the second, third and fourth branching levels have three channels per level. This configuration is the easiest among the other possible configurations to manufacture with only ten branching channels, one inlet, and three exits. This configuration also provides less fouling of the branching channels.

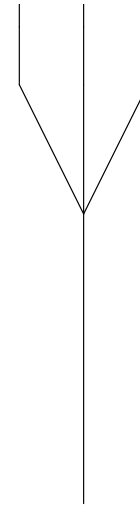


Fig. 21: Geometry of Pareto point 1 after 500 iterations with 4 branching levels.

The optimized results could be viewed from another angle by taking into consideration that at the present time it is expected from a cooling network to remove approximately 10 Watts per squared centimeters. Configuration of Pareto point 4 provides similar results to those expected. Since the surface area of the object where this particular fractal branching network can be implemented is 18 cm², 3 cm wide by 6 cm long, it is expected that this network removes approximately 180 Watts of heat. The configuration of Pareto point number 4 provides a similar amount of total heat removed with 188.21 Watts. This configuration is presented in Figure 22.

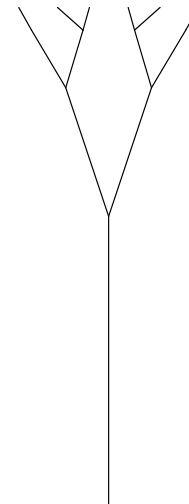


Fig. 22: Geometry of Pareto point 4 after 500 iterations with 4 branching levels.

Thus, the configuration of Pareto point 4, represented in Figures 18, 19, and 20 as the fourth point from left to right, provides approximately 14 times total heat removed per each Watt of pumping power necessary. Figure 20 further enhances this observation by noticing that for the fourth point from left to right the amount of pumping power necessary is approximately

13 Watts and the amount of total heat removed is approximately 188 Watts.

Of particular interest is the optimal design of Pareto point 56 for which the amount of thermal energy removed equals the amount of energy spent on facilitating this removal. For optimum design No. 56 the amount of thermal energy removed is 494 Watts, which is approximately half of the maximum possible, 990 Watts for the initial configuration, while requiring only 16% of the original total pressure drop and only 40% of the original mass flow rate. Topology of the branching channels for the optimized design No. 56 is depicted in Figure 23.

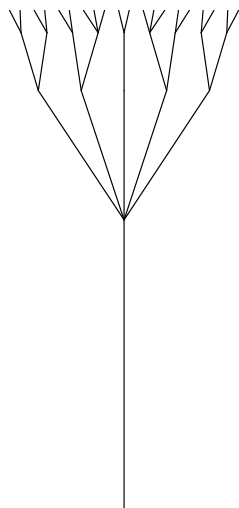


Fig. 23: Geometry of Pareto point 56 after 500 iterations with 4 branching levels.

CONCLUSIONS

A complete methodology for preliminary design optimization, of fractal branching channel networks of internal cooling passages utilizing a compressible homo-compositional fluid, has been described and demonstrated. A complete software package was developed for affordable preliminary design optimization of fractal branching channel networks of cooling passages with multiple simultaneous objectives. The software package includes: a random branches generator, a multi-objective hybrid optimizer, COOLNET (quasi 1-D thermo-fluid analysis code), program OBJ, analyzer and a program to visualize the geometry of the branches.

The analysis described in this work can be applied whenever a cooling problem requires optimization, to obtain a better design. This analysis helps the user to easily identify which design is the best for the desired needs. As the result of this analysis one design is chosen as the best one among other designs obtained from the optimizer's output file depending of the desired application. In this work the total number of design options was one hundred Pareto points.

The magnitudes of the heat transfer to total pressure drop ratio and heat transfer to pumping power ratio can be increased by incorporating the channels' hydraulic diameter, cross sectional area, lengths, and wall roughness as optimization variables. Future work in this area may include branching networks with more branching levels, and include the wall roughness, hydraulic diameters, cross sectional areas of the channels and branches lengths, as design variables.

REFERENCES

1. Martin, T. J., 2001, "Computer-Automated Multi-Disciplinary Analysis and Design Optimization of Internally Cooled Turbine Blades," Ph.D. Dissertation, Department of Aerospace Engineering, The Pennsylvania State University, University Park, PA.
2. Martin, T. J. and Dulikravich, G. S., 2001, "Aero-Thermo-Elastic Inverse Design and Optimization of Internally Cooled Turbine Blades," Chapter 5 in *Coupled Field Problems, Series on Advances in Boundary Elements*, (eds: Aliabadi, M. H. and Kassab, A. J.), WIT Press, Boston, MA, pp. 137-184.
3. Martin, T. J. and Dulikravich, G. S., 2002, "Analysis and Multi-Disciplinary Optimization of Internal Coolant Networks in Turbine Blades," *AIAA Journal of Propulsion and Power*, Vol. 18, No. 4, pp. 896-906.
4. Moaveni, S., 2003, "Finite element analysis: theory and application with ANSYS," 2nd Edition, Pearson Education, Upper Saddle River, NJ.
5. Reddy, J. N. and Gartling, D. K., 2000, *The Finite Element Method in Heat Transfer and Fluid Dynamics*, 2nd Edition, CRC Press, Boca Raton, FL.
6. Carey, G. F. and Oden, J. T., 1986, *Finite Elements: Fluid Mechanics, Vol. VI*, Prentice Hall, Englewood Cliffs, NJ.
7. Dulikravich, G. S., Moral, R. and Sahoo, D., 2005, "A Multi-Objective Evolutionary Hybrid Optimizer," EUROGEN 05 - Evolutionary and Deterministic Methods for Design, Optimization and Control with Applications to Industrial and Societal Problems, (eds: R. Schilling, W. Haase, J. Periaux, H. Baier, G. Bugeada), Munich, Germany, September 12-14, 2005.
8. Iorio, A. and Li, X., 2004, "Solving Rotated Multi-objective Optimization Problems Using Differential Evolution," Proceeding of the 17th Joint Australian Conference on Artificial Intelligence, Cairns, Australia.
9. Zitzler, E. and Thiele, L., 1999, "Multiobjective Evolutionary Algorithms: A Comparative Case Study and the Strength Pareto Approach," *IEEE Transactions on Evolutionary Computation*, Vol. 3, No. 4, pp. 257-271.
10. Eberhart, R., Shi, Y. and Kennedy, J., 2001, *Swarm Intelligence*, Morgan Kaufmann, San Francisco, CA.
11. Deb, K., 2002, "Multi-Objective Optimization Using Evolutionary Algorithms," John Wiley & Sons, Baffins Lane, Chichester, England, ISBN 047187339X.
12. Computer resource used for calculations, <http://maidroc.fiu.edu/>; date: 6/1/2005
13. Alharbi, A. Y., Pence, D. V. and Cullion, R. N., 2003, "Temperature Distributions in Microscale Fractal-like Branching Channel Networks," ASME paper HT2003-47501, ASME Summer Heat Transfer Conference, Las Vegas, NV, July 21-23, 2003.
14. Bejan, A., 1997, "Constructal Tree Network for Fluid Flow Between a Finite-Size Volume and One Source or Sink," *Revue Generale de Thermique*, Vol. 36, pp. 592-604.
15. West, G. B., Brown, J.H. and Enquist, B. J., 1997, "A General Model for the Origin of Allometric Scaling Laws in Biology," *Science*, 276, pp. 122-126.
16. Jelisavcic, N., Martin, T. J., Moral, R., Sahoo, D., Dulikravich, G. S. and Gonzalez, M., 2005, "Design Optimization of Networks of Cooling Passages," ASME paper IMECE2005-17195, Orlando, FL, Nov. 5-11, 2005.